Journal of Marine Science and Application (2019) 18:542–553
https://doi.org/10.1007/s11804-019-00103-8

RESEARCH ARTICLE

A Strong Tracking Filtering Approach for Health Estimation of Marine Gas Turbine Engine

Qingcai Yang[1] · Shuying Li[1] · Yunpeng Cao[1]

Received: 30 March 2018 / Accepted: 25 June 2018 / Published online: 23 August 2019

Abstract
Monitoring and evaluating the health parameters of marine gas turbine engine help in developing predictive control techniques and maintenance schedules. Because the health parameters are unmeasurable, researchers estimate them only based on the available measurement parameters. Kalman filter-based approaches are the most commonly used estimation approaches; however, the conventional Kalman filter-based approaches have a poor robustness to the model uncertainty, and their ability to track the mutation condition is influenced by historical data. Therefore, in this paper, an improved Kalman filter-based algorithm called the strong tracking extended Kalman filter (STEKF) approach is proposed to estimate the gas turbine health parameters. The analytical expressions of Jacobian matrixes are deduced by non-equilibrium point analytical linearization to address the problem of the conventional approaches. The proposed approach was used to estimate the health parameters of a two-shaft marine gas turbine engine in the simulation environment and was compared with the extended Kalman filter (EKF) and the unscented Kalman filter (UKF). The results show that the STEKF approach not only has a computation cost similar to that of the EKF approach but also outperforms the EKF approach when the health parameters change abruptly and the noise mean value is not zero.

Keywords Gas turbine · Health parameter estimation · Extended Kalman filter · Unscented Kalman filter · Strong tracking Kalman filter · Analytical linearization

1 Introduction

As the service life of a gas turbine increases, its performance degrades due to the degradation of its components, such as the compressor, combustion chamber, and turbine. Causes of the components degradation include fouling, erosion, corrosion, and foreign object damage, which can cause gradual or abrupt variation in the gas turbine performance (Volponi 2013). Performance degradation decreases the gas turbine stability, increases fuel consumption, decreases fuel economy, and increases operating costs. Therefore, monitoring and evaluating the gas turbine performance are important. The health parameters usually refer to the component corrected mass flow and isentropic efficiency, which will change with the gas turbine performance degradation. Monitoring and estimating changes in gas turbine health parameters can help in developing predictive control techniques and maintenance schedules to improve the gas turbine performance. However, the health parameters cannot be directly measured, and they can only be obtained by estimation techniques on the basis of the available measurement parameters data (Li 2010).

For estimating health parameters, various estimation approaches have been proposed, such as weighted least squares approach (Li and Korakiantis 2012), optimization approach (Li and Pilidis 2010; Yang et al. 2014), Kalman filter and its derivative approaches (Kerr et al. 1992; Simon and Simon 2005; 2006; 2010; Simon and Garg2010), nonlinear filtering approach (Simon 2006), and observer approach (Chang et al. 2016). Health parameter estimation based on Kalman filter is

Article Highlights
- An improved strong tracking extended Kalman filter approach is proposed to estimate marine gas turbine health parameters in uncertainty and mutation condition.
- The analytical expression of Jacobian matrix is deduced by non-equilibrium point analytical linearization.
- The proposed method is compared with the extended Kalman filter (EKF) and the unscented Kalman filter (UKF).

✉ Yunpeng Cao
caoyunpeng@hrbeu.edu.cn

[1] College of Power and Energy Engineering, Harbin Engineering University, Harbin 150001, China

the most commonly used approach. A large number of Kalman filter-based approaches have been proposed, and they have achieved good results in practical applications (Kobayashi et al. 2005; Brotherton et al. 2003). Common variants of the Kalman filter include the linearized Kalman filter (LKF), extended Kalman filter (EKF), and unscented Kalman filter (UKF).

The LKF is the earliest and the most widely used for gas turbine health parameters estimation because of its low computational cost (Simon 2008). Luppold et al. (1989) first proposed the use of Kalman filter for estimating aircraft performance changes. In 1991, Lambert designed a Kalman filter to estimate the efficiencies of low-pressure and high-pressure turbines. Kerr et al. (1992) described the second-generation Kalman filter algorithm for real-time estimation of gas turbine gas path damage. Considering that some prior knowledge is often neglected because it does not easily fit into the structure of the Kalman filter, to improve estimation accuracy, Simon and Simon (2005) proposed an estimation approach based on the constrained Kalman filter for turbofan. Then, this approach was improved using the probability density truncation (Simon and Simon 2010). For the underdetermined estimation problem, Simon and Garg (2010) proposed an optimal tuning parameter selection approach for estimating multiple health parameters.

Although the LKF has a low computational cost, local linearization will result in a non-negligible model error because the gas turbine is a nonlinear system, leading to large health parameters estimation errors. In addition, although the linear model accurately represents the gas turbine dynamics at a certain operating condition, it may not be accurate at other operating conditions. Therefore, a set of linear models corresponding to different operating conditions is required to represent the gas turbine dynamics at the entire operating range.

To reduce the linearization error and improve the estimation accuracy, nonlinear estimation approaches such as the EKF and UKF have been proposed. Kobayashi et al. (2005) proposed the constant gain extended Kalman filter approach for aircraft performance parameter estimation to improve accuracy while reducing computation cost. In addition, several researchers have compared different estimation approaches (Volponi et al. 2003; Simon 2008; Borguet and Léonard 2010; Lu et al. 2013). Simon (2008) compared the computational cost and the estimated accuracy of three commonly used Kalman filter approaches; the EKF and UKF showed similar performance, but the computational cost required by the UKF was an order of magnitude higher than that required by the EKF. Therefore, it appears that the EKF is the best choice for aircraft engine health parameter estimation (Simon 2008).

However, the EKF has a poor robustness to model uncertainties and a poor mutation condition tracking ability (Zhou and Frank 1996). The main factors causing model uncertainty include model simplification and inaccurate initial noise covariance matrixes. For the EKF, due to the local linearization, the model error increases, and as a result, the model uncertainty increases. In addition, the EKF is a recursive filter, and all the historical data influence the current estimates. The historical data affects the Kalman gain of the EKF; when the gas turbine is in steady state for a long time, the Kalman gain tends to be constant. For abrupt changes in the health parameter of the gas turbine, the EKF tracking ability of the mutation condition is poor, and the Kalman gain matrix changes slowly, which delays the health parameters estimation.

To overcome the abovementioned problems and improve the Kalman filter performance, Zhou and Frank (1996) proposed a strong tracking Kalman filter approach, which has been applied for gas turbine performance parameters estimation (Pu et al. 2013). By introducing the fading factor into the covariance matrix of state prediction, the Kalman gain matrix is adjusted on-line, and the output residual sequence is maintained orthogonal to make the filter robust to the model uncertainty and still keep track of the system state. The strong tracking filter (STF) has a strong robustness to system uncertainties: low sensitivity to system noise, measurement noise, and initial noise covariance matrixes as well as a strong ability to track the mutation state (Zhou and FRANK 1996).

In this paper, an improved Kalman filter-based approach called the strong tracking extended Kalman filter (STEKF) is proposed for health parameters estimation in the existence of model uncertainty and mutation condition. Since the STEKF approach also requires determining the Jacobian matrix, a Jacobian matrix determination approach based on non-equilibrium analytical linearization is proposed. By decomposing each of the gas turbine component models into several sub-modules, each sub-module was linearized separately. In the linearization process, the health parameters were extended to the state variables, and the intermediate variables were eliminated. Then, the analytical expression of Jacobian matrix was derived by symbolic calculation, and the Jacobian matrix was determined in real time. Finally, the STEKF and the conventional nonlinear filtering approaches, i.e., EKF and UKF, were used to estimate the health parameters in the simulation environment, and the three approaches were compared according to their estimated results.

This paper is organized as follows: The studied gas turbine nonlinear dynamic model and the typical gas path fault are briefly introduced in Section 2. Section 3 briefly introduces the current Kalman filter-based gas turbine health parameter estimation approach. Section 4 describes the Jacobi matrix determination approach based on non-equilibrium point analytical linearization. The estimation results of the three nonlinear filtering approaches are compared in detail under different situations in Section 5. The conclusions are presented in Section 6.

2 Nonlinear Dynamic Model of Gas Turbine

In this study, a two-shaft marine gas turbine was investigated. For a two-shaft gas turbine, the main components include a compressor, a combustion chamber, a compressor turbine, and a power turbine, whereby the power turbine drives the propeller through the reduction gearbox. The simplified layout of the gas turbine is shown in Fig. 1, in which the reduction gearbox and propeller are simplified as a load.

Based on the literature on the nonlinear dynamic modeling of a gas turbine (Klapproth et al. 1979; Camporeale et al. 2006; Tsoutsanis et al. 2013; Yang et al. 2017), in the present study, a General Electric LM2500 simulation model was established in MATLAB/Simulink environment. To simulate the nonlinear dynamic response of the gas turbine, rotor dynamics and volume dynamics were considered. The heat transfer dynamics also affects the nonlinear dynamic response, especially in the start-up or shutdown process. However, this study is mainly focused on a gas turbine in operation; therefore, heat transfer dynamics was neglected due to its low influence on gas turbine dynamic response during operation. Thus, the nonlinear set of governing equations of motion for the marine gas turbine can be described as follows:

$$
\begin{aligned}
\dot{N}_l &= \left[\frac{30}{\pi}\right]^2 \frac{1}{J_1 N_l}\left[m_h \eta_m c_{pg}(T_3 - T_4) - m_c c_p (t_2 - T_1)\right] \\
\dot{N}_P &= \left[\frac{30}{\pi}\right]^2 \frac{1}{J_2 N_P}\left[m_p c_{pg}(T_4 - T_5) - \mathrm{KN}_P^3\right] \\
\dot{T}_3 &= \frac{R_g T_3}{P_3 V_1 c_{vg}}\left[k\left(c_{pg} T_2 m_c + \mathrm{LHV}\eta_b w_f - c_{pg} T_3 m_h\right) - \right. \\
&\qquad \left. c_{pg} T_3\left(m_c + m_f - m_h\right)\right] \qquad (1) \\
\dot{P}_3 &= \frac{P_3}{T_3}\dot{T}_3 + \frac{\mathrm{RT}_3\left(m_c + w_f - m_h\right)}{V_1} \\
\dot{P}_4 &= \frac{\left(m_h - m_p\right)\mathrm{RT}_4}{V_2} \\
P_5 &= \frac{\left(m_5 - \kappa\sqrt{P_5}\right)\mathrm{RT}_5}{V_3}
\end{aligned}
$$

where η_m denotes mechanical efficiency; J_1 and J_2 denote the inertia of the compressor shaft and power turbine shaft, respectively; K denotes the coefficient of the relationship between the power turbine rotational speed and the load power; LHV denotes the fuel low calorific value; V_1, V_2, and V_3 denote the component volume; and κ denotes the relationship between mass flow and pressure.

Gas turbine failure occurs during operation, and common faults include fouling, erosion, corrosion, and foreign objects damage. These faults change the structure of components, thereby changing the characteristics map, and then, the gas turbine performance degrades, resulting in changes in gas turbine health parameters. These health parameters are generally the corrected mass flow and the isentropic efficiency of the components (Pu et al. 2013). This study mainly considers the following six health parameters: (1) change in compressor corrected mass flow, H_{mc}; (2) change in compressor isentropic efficiency, $H_{\eta\mathrm{c}}$; (3) change in high-pressure turbine corrected mass flow, H_{mct}; (4) change in high-pressure turbine isentropic efficiency, $H_{\eta\mathrm{ct}}$; (5) change in power turbine corrected mass flow, H_{mpt}; and (6) change in power turbine isentropic efficiency, $H_{\eta\mathrm{pt}}$.

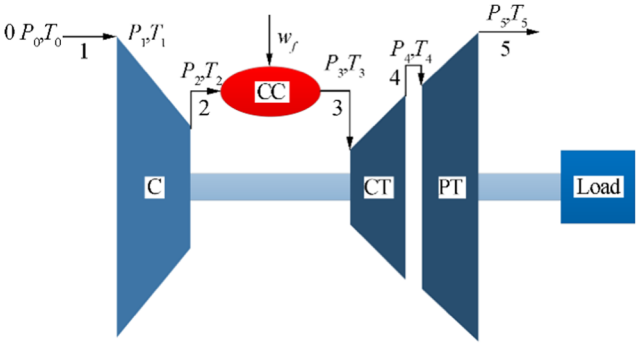

Fig. 1 Schematic of a two-shaft gas turbine engine

Here, H denotes health parameters. When the gas turbine is in a healthy condition, the corresponding health parameter is equal to 1, while in the presence of a fault, the health parameter is not equal to 1. For example, $H_{\mathrm{mc}} < 1$ indicates a compressor fault has occurred and caused a decrease in the compressor corrected mass flow.

3 Nonlinear Approaches for Health Parameters Estimation

This section briefly describes the nonlinear approaches for estimating gas turbine health parameters. The LKF-based estimation approach can obtain the optimal state estimation for linear Gaussian systems with low computation cost (Simon 2008). However, because the gas turbine is a nonlinear system, linearization will lead to a non-negligible model error and increase the estimation error. Moreover, it is necessary to establish a piecewise linear model to estimate the health parameters under different operating conditions. Therefore, to reduce the error introduced by linearization, nonlinear estimation approaches, such as the EKF and UKF approaches, have been proposed.

However, the conventional nonlinear Kalman filter approach has a poor robustness to the model uncertainties and a poor ability for tracking mutation condition. Considering the existing problems of the conventional Kalman filter approach, Zhou and FRANK (1996) proposed the STF algorithm. The STF has a strong robustness to system uncertainties; low sensitivity to system noise, measurement noise, and initial noise covariance matrixes; as well as strong ability to track the

mutation state. Therefore, the STF is more effective for estimating gas turbine health parameters.

In this study, the STEKF, which based on the EKF, was designed to estimate the gas turbine performance parameters. Considering the discrete-time nonlinear system is shown in Eq. (2).

$$\begin{aligned} \boldsymbol{x}_k &= f(\boldsymbol{x}_{k-1}, \boldsymbol{u}_{k-1}) + \boldsymbol{w}_{k-1} \\ \boldsymbol{y}_{k-1} &= h(\boldsymbol{x}_{k-1}) + \boldsymbol{v}_{k-1} \end{aligned} \tag{2}$$

Here, $\boldsymbol{x}$ denotes the state variable, $\boldsymbol{u}$ denotes the control variable, $\boldsymbol{y}$ denotes the output variable, and $\boldsymbol{w}$ and $\boldsymbol{v}$ denote the process noise and the measurement noise, respectively, where both are the zero-mean Gaussian noise, and the corresponding covariance matrixes are $\boldsymbol{Q}$ and $\boldsymbol{R}$, respectively.

Compared with the EKF, the main improvement of the STEKF is the introduction of the suboptimal fading factor in the estimation error covariance matrix (Pu et al. 2013). The factor is assumed to be λ_{k-1}, as shown in Eq. (3).

$$\boldsymbol{P}_k = \lambda_{k-1}\boldsymbol{A}\boldsymbol{P}_{k-1}^{+}\boldsymbol{A}^{\mathrm{T}} + \boldsymbol{Q} \tag{3}$$

The suboptimal fading factor can be recursively solved by Eq. (4)

$$\begin{aligned} &E\left[\left(\boldsymbol{x}_k^{+} - \hat{\boldsymbol{x}}\right)\left(\boldsymbol{x}_k^{+} - \hat{\boldsymbol{x}}\right)^{\mathrm{T}}\right] = \min \\ &E\left[\left(\boldsymbol{y}_k\right)^{\mathrm{T}}\left(\boldsymbol{y}_{k+1+j}\right)\right] = 0, k = 0, 1, 2, ..., j = 1, 2, ... \end{aligned} \tag{4}$$

The second equation in Eq. (4) is called the orthogonality principle, which holds that the residual error series should be made mutually orthogonal at each step, and this makes the filter robust to the model uncertainty. The STEKF algorithm is shown in Table 1, and more detailed information can be found in the work of Zhou and FRANK (1996).

To evaluate the STEKF performance in the health parameters estimation, the STEKF was compared with the commonly used nonlinear estimation approaches (EKF and UKF). Tables 2 and 3 briefly describe the EKF and UKF algorithms, respectively. More detailed information can be found in the work of Simon (2008).

Table 1 Strong tracking extended Kalman filter algorithm

The prediction step

$$\hat{\boldsymbol{x}}_k = f\left(\hat{\boldsymbol{x}}_{k-1}^{+}, \boldsymbol{u}_{k-1}\right)$$

$$\boldsymbol{P}_k = \lambda_{k-1}\boldsymbol{A}\boldsymbol{P}_{k-1}^{+}\boldsymbol{A}^{\mathrm{T}} + \boldsymbol{Q}$$

The measurement update step

$$\boldsymbol{K}_k = \boldsymbol{P}_k\boldsymbol{C}^{\mathrm{T}}\left(\boldsymbol{C}\boldsymbol{P}_k\boldsymbol{C}^{\mathrm{T}} + \boldsymbol{R}\right)^{-1}$$

$$\gamma_k = \boldsymbol{y}_k - h(\hat{\boldsymbol{x}}_k)$$

$$\hat{\boldsymbol{x}}_k^{+} = \hat{\boldsymbol{x}}_k + \boldsymbol{K}_k\gamma_k$$

$$\boldsymbol{P}_k^{+} = (\boldsymbol{I} - \boldsymbol{K}_k\boldsymbol{C})\boldsymbol{P}_k$$

$$\lambda_k = \begin{cases} \lambda_0, & \lambda_0 \geq 1 \\ 1, & \lambda_0 < 1 \end{cases}$$

$$\lambda_0 = \frac{tr[\boldsymbol{N}_k]}{tr[\boldsymbol{M}_k]}$$

$$\boldsymbol{N}_k = \boldsymbol{V}_k^0 - \boldsymbol{C}\boldsymbol{Q}\boldsymbol{C}^{\mathrm{T}} - \beta\boldsymbol{R}$$

$$M_k = \boldsymbol{C}\boldsymbol{A}\boldsymbol{P}_{k-1}^{+}\boldsymbol{A}^{\mathrm{T}}\boldsymbol{C}^{\mathrm{T}}$$

$$\boldsymbol{V}_k^0 = \begin{cases} \gamma_1(\gamma_1)^{\mathrm{T}}, & k = 0 \\ \dfrac{\rho\boldsymbol{V}_{k-1}^0 + \gamma_k(\gamma_k)^{\mathrm{T}}}{1+\rho}, & k \geq 1 \end{cases}$$

Notation

$$\boldsymbol{A} = \frac{\partial f\left(\hat{\boldsymbol{x}}_{k-1}^{+}, \boldsymbol{u}_{k-1}\right)}{\partial x}$$

$$\boldsymbol{C} = \frac{\partial h(\hat{\boldsymbol{x}}_k)}{\partial x}$$

$tr[\cdot]$ denotes the trace of a matrix

ρ denotes forgetting factor

β denotes softening factor

4 Jacobian Matrix Determination Based on Analytical Linearization

In this study, the STEKF was designed based on the EKF; therefore, Jacobian matrixes calculation is needed at each filtering step. However, for the gas turbine, the calculation of Jacobian matrix is complicated, as it is usually periodically updated or done directly offline, and this increases the estimation error (Kobayashi et al. 2005). To overcome this problem, non-equilibrium analytic linearization is used to derive the analytical expression of the Jacobian matrix under the non-equilibrium point.

Figure 2 shows the modules and the information flows in the Simulink gas turbine nonlinear dynamic model. Each component is decomposed into several sub-modules, and each sub-module is composed of a nonlinear equation. The compressor, for example, contains the temperature sub-module, the corrected mass flow sub-module, and the isentropic efficiency sub-module. Each sub-module is linearized, and the linearization model of the component can be derived from symbolic computation according to the information flows among sub-modules. Then, the analytical expressions of Jacobian matrixes are deduced, which are used to estimate the health parameters based on the STEKF algorithm.

4.1 Non-equilibrium Linearization

Considering the change of the gas turbine health parameters and assuming that the change rate of the health parameters is zero (Pu et al. 2013), Eq. (1) can be changed to a nonlinear system as shown in Eq. (5)

$$\begin{aligned} \dot{\boldsymbol{x}} &= f(x, \boldsymbol{H}, \boldsymbol{u}) + \boldsymbol{w} \\ \boldsymbol{y} &= h(\boldsymbol{x}, \boldsymbol{H}) + \boldsymbol{v} \end{aligned} \tag{5}$$

Table 2 Extended Kalman filtering algorithm

The prediction step

$$\hat{\boldsymbol{x}}_k = f\left(\hat{\boldsymbol{x}}_{k-1}^{+}, \boldsymbol{u}_{k-1}\right)$$
$$\boldsymbol{P}_k = \boldsymbol{A}\boldsymbol{P}_{k-1}^{+}\boldsymbol{A}^{\mathrm{T}} + \boldsymbol{Q}$$

The measurement update step

$$\boldsymbol{K}_k = \boldsymbol{P}_k\boldsymbol{C}^{\mathrm{T}}\left(\boldsymbol{C}\boldsymbol{P}_k\boldsymbol{C}^{\mathrm{T}} + \boldsymbol{R}\right)^{-1}$$
$$\boldsymbol{\gamma}_k = \boldsymbol{y}_k - h(\hat{\boldsymbol{x}}_k)$$
$$\hat{\boldsymbol{x}}_k^{+} = \hat{\boldsymbol{x}}_k + \boldsymbol{K}_k\boldsymbol{\gamma}_k$$
$$\boldsymbol{P}_k^{+} = (\boldsymbol{I} - \boldsymbol{K}_k\boldsymbol{C})\boldsymbol{P}_k$$

Notation

$$\boldsymbol{A} = \frac{\partial f\left(\hat{\boldsymbol{x}}_{k-1}^{+}, \boldsymbol{u}_{k-1}\right)}{\partial x}$$
$$\boldsymbol{C} = \frac{\partial h(\hat{\boldsymbol{x}}_k)}{\partial x}$$

Here, $\boldsymbol{x}$ denotes the state variable, $\boldsymbol{x} = [N_l, N_p, T_3, P_3, P_4, P_5]^{\mathrm{T}}$; $\boldsymbol{u}$ denotes the control variable, $\boldsymbol{u} = w_f$; $\boldsymbol{y}$ denotes the output variable, $\boldsymbol{y} = [N_l, N_p, T_2, P_2, T_4, P_4, T_5, P_5]^{\mathrm{T}}$; H denotes health parameters, $\boldsymbol{H} = [H_{\mathrm{mc}}, H_{\eta\mathrm{c}}, H_{\mathrm{mcT}}, H_{\eta\mathrm{cT}}, H_{\mathrm{mpT}}, H_{\eta\mathrm{pT}}]^{\mathrm{T}}$; and w and v denote the process noise and measurement noise, respectively, where both noises are the zero-mean Gaussian noise, and the corresponding covariance matrixes are $\boldsymbol{Q}$ and $\boldsymbol{R}$, respectively.

At any point $(\boldsymbol{x}_i,\boldsymbol{H}_i,\boldsymbol{u}_i)$, Taylor expansion is performed on Eq. (5), and the high-order terms are ignored. A linearization model as shown in Eq. (6) can be obtained (Johansen et al. 1998):

$$\begin{aligned}\dot{\boldsymbol{x}} &= f(\boldsymbol{x}_i, \boldsymbol{H}_i, \boldsymbol{u}_i) + \boldsymbol{L}_i\Delta\boldsymbol{x} + \boldsymbol{M}_i\Delta\boldsymbol{H} + \boldsymbol{N}_i\Delta\boldsymbol{u} \\ \boldsymbol{y} &= h(\boldsymbol{x}_i, \boldsymbol{H}_i) + \boldsymbol{E}_i\Delta\boldsymbol{x} + \boldsymbol{F}_i\Delta\boldsymbol{H}\end{aligned} \tag{6}$$

where

$$\boldsymbol{L}_i = \frac{\partial f}{\partial x}(\boldsymbol{x}_i, \boldsymbol{H}_i, \boldsymbol{u}_i), \boldsymbol{M}_i = \frac{\partial f}{\partial H}(\boldsymbol{x}_i, \boldsymbol{H}_i, \boldsymbol{u}_i)$$
$$\boldsymbol{N}_i = \frac{\partial f}{\partial u}(\boldsymbol{x}_i, \boldsymbol{H}_i, \boldsymbol{u}_i), \boldsymbol{E}_i = \frac{\partial h}{\partial x}(\boldsymbol{x}_i, \boldsymbol{H}_i), \boldsymbol{F}_i = \frac{\partial h}{\partial H}(\boldsymbol{x}_i, \boldsymbol{H}_i)$$

Here, $f(\boldsymbol{x}_{\mathrm{i}},\boldsymbol{H}_{\mathrm{i}},\boldsymbol{u}_{\mathrm{i}})$ represents the function value of $f(\boldsymbol{x},\boldsymbol{H},\boldsymbol{u})$ at point $(\boldsymbol{x}_{\mathrm{i}},\boldsymbol{H}_{\mathrm{i}},\boldsymbol{u}_{\mathrm{i}})$, and similarly, $h(\boldsymbol{x}_{\mathrm{i}},\boldsymbol{H}_{\mathrm{i}})$ represents the function value of $h(\boldsymbol{x},\boldsymbol{H})$ at point $(\boldsymbol{x}_{\mathrm{i}},\boldsymbol{H}_{\mathrm{i}},\boldsymbol{u}_{\mathrm{i}})$. These values are zero when the gas turbine is operating at steady state and non-zero during transition. Equation (6) can be rewritten as Eq. (7):

$$\begin{aligned}\begin{bmatrix}\dot{\boldsymbol{x}} \\ \dot{\boldsymbol{H}}\end{bmatrix} &= \begin{bmatrix}\boldsymbol{L}_i & \boldsymbol{M}_i \\ 0 & 0\end{bmatrix}\begin{bmatrix}\boldsymbol{x} \\ \boldsymbol{H}\end{bmatrix} + \begin{bmatrix}\boldsymbol{N}_i \\ 0\end{bmatrix}\boldsymbol{u} + \begin{bmatrix}\boldsymbol{d}_i \\ 0\end{bmatrix} \\ \boldsymbol{y} &= [\boldsymbol{E}_i \;\; \boldsymbol{F}_i]\begin{bmatrix}\boldsymbol{x} \\ \boldsymbol{H}\end{bmatrix} + \boldsymbol{e}_i\end{aligned} \tag{7}$$

where

$$\boldsymbol{d}_i = f(\boldsymbol{x}_i, \boldsymbol{H}_i, \boldsymbol{u}_i) - \boldsymbol{L}_i\boldsymbol{x}_i - \boldsymbol{M}_i\boldsymbol{H}_i - \boldsymbol{N}_i\boldsymbol{u}_i$$
$$\boldsymbol{e}_i = h(\boldsymbol{x}_i, \boldsymbol{H}_i) - \boldsymbol{E}_i\boldsymbol{x}_i - \boldsymbol{F}_i\boldsymbol{H}_i$$

Therefore, the Jacobian matrix is

$$\boldsymbol{A} = \begin{bmatrix}\boldsymbol{L}_i & \boldsymbol{M}_i \\ 0 & 0\end{bmatrix}, \boldsymbol{C} = [\boldsymbol{E}_i \;\; \boldsymbol{F}_i]$$

The Jacobian matrixes are dynamic matrixes that change with the condition of the gas turbine, and it is determined by the parameters of the gas turbine nonlinear model; therefore, if the analytical expression of the Jacobian matrix is determined, the Jacobian matrix can be quickly determined based on the nonlinear model current parameters. In addition, the linearization process indicates that either under the equilibrium or non-equilibrium point, the analytical expressions of Jacobian matrix are the same; therefore, the analytical expression of the Jacobian matrix can be directly derived under equilibrium point, and then, the Jacobian matrix is obtained under non-equilibrium point.

4.2 Jacobian Matrix

The problem of determining the Jacobian matrixes through the analytical linearization approach is that this approach can only be performed for expressions; however, the component map in the model is usually expressed by a look-up table; therefore, the analytical linearization approach cannot be directly performed. In this study, the central difference approach is used to realize the analytical linearization of the component map by converting the differential to the difference. Since the component performance deterioration can be considered to be caused by a change in the component map, the component map can be considered to be a function of the health parameter, as shown in Eq. (8).

$$\begin{cases} m = f_m(N, \pi, H_m) \\ \eta = f_\eta(m, N, H_\eta) \end{cases} \tag{8}$$

Using the central difference approach, Eq. (8) is linearized, as shown in Eq. (9).

$$\begin{cases} \Delta m_{\mathrm{Act}} = \boldsymbol{D}_m\Delta\boldsymbol{u}_m \\ \Delta\eta_{\mathrm{Act}} = \boldsymbol{D}_\eta\Delta\boldsymbol{u}_\eta \end{cases} \tag{9}$$

where $\boldsymbol{D}_m$ and $\boldsymbol{D}_\eta$ denote the linearization matrix, and $\boldsymbol{u}_m = [N\ \pi\ H_m]^{\mathrm{T}}$, $\boldsymbol{u}_\eta = [m\ N\ H_\eta]^{\mathrm{T}}$.

For the other sub-modules shown in Fig. 2, they can be directly linearized. For the component linearization model, the derivation can be made by symbolic calculation through the relationship among the sub-modules that form the component model. The nonlinear equation shown in Eq. (1) can be

Table 3 Unscented Kalman filtering algorithm

Initialization

$$\boldsymbol{x}_0^+ = E[\boldsymbol{x}_0]$$
$$\boldsymbol{P}_0^+ = E\left[\left(\boldsymbol{x}_0 - \boldsymbol{x}_0^+\right)\left(\boldsymbol{x}_0 - \boldsymbol{x}_0^+\right)^{\mathrm{T}}\right]$$

The prediction step

Sigma point

$$\boldsymbol{x}_{k-1}^{(i)} = \boldsymbol{x}_{k-1}^+ + \boldsymbol{x}\sim^{(i)}, i = 1, \cdots, 2n$$
$$\boldsymbol{x}\sim^{(i)} = \left(\sqrt{(n+\lambda)\boldsymbol{P}_{k-1}^+}\right)_i, i = 1, \cdots, n$$
$$\boldsymbol{x}\sim^{(n+i)} = -\left(\sqrt{(n+\lambda)\boldsymbol{P}_{k-1}^+}\right)_i, i = 1, \cdots, n$$

Time update

$$\hat{\boldsymbol{x}}^{(i)}{}_k = f\left(\hat{\boldsymbol{x}}^{(i)}{}_{k-1}, \boldsymbol{u}_{k-1}\right)$$
$$\hat{\boldsymbol{x}}_k = \frac{1}{2n}\sum_{i=0}^{2n} \boldsymbol{w}_i^m \hat{\boldsymbol{x}}^{(i)}{}_k$$
$$\boldsymbol{P}_{xk} = \frac{1}{2n}\sum_{i=0}^{2n} \boldsymbol{w}_i^c \left[\left(\hat{\boldsymbol{x}}_k^{(i)} - \hat{\boldsymbol{x}}_k\right)\left(\hat{\boldsymbol{x}}^{(i)}{}_k - \hat{\boldsymbol{x}}_k\right)^T\right] + \boldsymbol{Q}$$

The measurement update step

Sigma point

$$\boldsymbol{x}_k^{(i)} = \hat{\boldsymbol{x}}_k + \boldsymbol{x}\sim^{(i)}, i = 1, \cdots, 2n$$
$$\boldsymbol{x}\sim^{(i)} = \left(\sqrt{(n+\lambda)P_k}\right)_i, i = 1, \cdots, n$$
$$\boldsymbol{x}\sim^{(n+i)} = -\left(\sqrt{(n+\lambda)\boldsymbol{P}_k}\right)_i, i = 1, \cdots, n$$

Measurement update

$$\hat{\boldsymbol{y}}_k^{(i)} = h\left(\boldsymbol{x}_k^{(i)}\right)$$
$$\hat{\boldsymbol{y}}_k = \frac{1}{2n}\sum_{i=0}^{2n} \boldsymbol{w}_i^m \hat{\boldsymbol{y}}_k^{(i)}$$
$$\boldsymbol{P}_{yk} = \frac{1}{2n}\sum_{i=0}^{2n} \boldsymbol{w}_i^c \left[\left(\hat{\boldsymbol{y}}_k^{(i)} - \hat{\boldsymbol{y}}_k\right)\left(\hat{\boldsymbol{y}}_k^{(i)} - \hat{\boldsymbol{y}}_k\right)^T\right] + \boldsymbol{R}$$
$$\boldsymbol{P}_{xyk} = \frac{1}{2n}\sum_{i=0}^{2n} \boldsymbol{w}_i^c \left[\left(\hat{\boldsymbol{x}}^{(i)}{}_k - \hat{\boldsymbol{x}}_k\right)\left(\hat{\boldsymbol{y}}_k^{(i)} - \hat{\boldsymbol{y}}_k\right)^T\right]$$
$$\boldsymbol{K}_k = \boldsymbol{P}_{xyk}\left(\boldsymbol{P}_{yk}\right)^{-1}$$
$$\hat{\boldsymbol{x}}^+{}_k = \hat{\boldsymbol{x}}_k + \boldsymbol{K}_k\left(\boldsymbol{y}_k - \hat{\boldsymbol{y}}_k\right)$$
$$\boldsymbol{P}_k^+ = \boldsymbol{P}_k - \boldsymbol{K}_k \boldsymbol{P}_{yk}\left(\boldsymbol{K}_k\right)^T$$

Notation

$\left(\sqrt{\boldsymbol{A}}\right)_i$ denotes the ith row of $\sqrt{\boldsymbol{A}}$

n is the dimension of the state

$$\boldsymbol{w}_0^m = \frac{\lambda}{\lambda + n}$$
$$\boldsymbol{w}_0^c = \frac{\lambda}{\lambda + n} + \left(1 + \alpha^2 + \beta\right)$$
$$\boldsymbol{w}_i^m = w_i^c = \frac{1}{2(\lambda + n)}$$
$$\lambda = \alpha^2(n + k) - n$$
$$\alpha = 0.001; k = 0; \beta = 2$$

linearized, and the intermediate variable of Eq. (1) can be eliminated according to the relationship among the components, as shown in Fig. 2. The compressor rotor dynamics can be linearized by the compressor linearization model and the compressor turbine linearization model, and the power turbine rotor dynamics can be linearized by the power turbine linearization model. The combustion volume dynamic can be linearized by the compressor linearization model. The volume

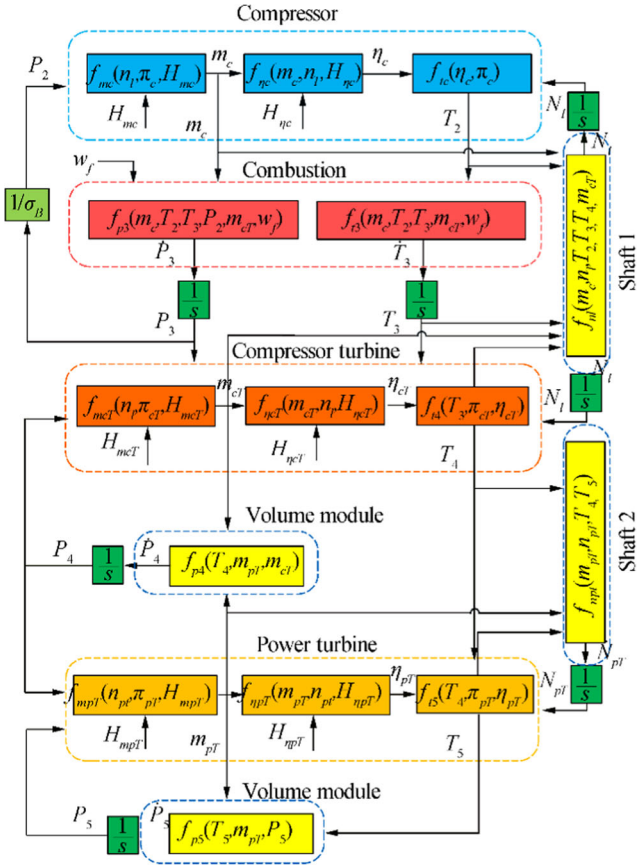

Fig. 2 Modules and the information flow of the gas turbine nonlinear mathematical model

module behind the compressor turbine can be linearized by the compressor turbine and the power turbine linearization models, and the volume module after power turbine is linearized by the power turbine linearization model. The outlet pressure of the compressor is obtained by the total pressure recovery coefficient and the outlet pressure of the combustion chamber, and the total pressure recovery coefficient is assumed to be constant.

The analytical linearization equation for Eq. (1) at any point is shown in Eq. (10)

$$\begin{aligned}
\dot{T}_3 &= A_{t3}T_3 + B_{t3}u_{t3} + \dot{T}_{3i} - A_{t3}T_{3i} - B_{t3}u_{t3i} \\
\dot{P}_3 &= A_{p3}P_3 + B_{p3}u_{p3} + \dot{P}_{3i} - A_{p3}P_{3i} - B_{p3}u_{p3i} \\
\dot{P}_4 &= B_{p4}u_{p4} + \dot{P}_{4i} - B_{p4}u_{p4i} \\
\dot{P}_5 &= A_{p5}P_5 + B_{p5}u_{p5} + \dot{P}_{5i} - A_{p5}P_{5i} - B_{p5}u_{p5i} \\
\dot{N}_l &= A_{\mathrm{nl}}\Delta n_l + B_{\mathrm{nl}}\Delta u_{\mathrm{nl}} + \dot{N}_{\mathrm{li}} - A_{\mathrm{nl}}\Delta n_{\mathrm{li}} - B_{\mathrm{nl}}\Delta u_{\mathrm{nli}} \\
\dot{N}_P &= A_{\mathrm{np}}\Delta n_p + B_{\mathrm{np}}\Delta u_{\mathrm{np}} + \dot{N}_{\mathrm{Pi}} - A_{\mathrm{np}}\Delta n_{\mathrm{pi}} - B_{\mathrm{np}}\Delta u_{\mathrm{npi}}
\end{aligned} \tag{10}$$

where u contains state variables, health parameters, and control variables. By rewriting Eq. (10) as a state space model, the variables are divided into two sets: one set of state variables and health parameters and another set of control variable. In this paper, there are six state variables

and a total of six health parameters, and the control variable is fuel flow.

Similarly, according to Fig. 2, the linearization equation of the measurement parameters can be derived from the analytical linearization approach. Thus, the analytical expression as shown in Eq. (7) can be obtained. The analytical linearization process indicates that the analytical expression of the Jacobian matrix does not change with the operating conditions, but the Jacobian matrix will vary with the operating conditions since it is a function of the gas turbine model parameters.

5 Results and Discussion

In practice, gas turbine failure can be divided into two categories. One is the gradual faults, such as fouling, erosion, and corrosion, which degrade the gas turbine performance, and in this case, the health parameters gradually change over time. Another category is the abrupt faults, such as blade fracture and foreign objects damage; in this case, the health parameters change abruptly. The variation value of the health parameters caused by the two failure categories may be large or small. In this study, to simulate these two categories, the gradual and abrupt variations of the different health parameters were considered and with different amplitudes. In addition, steady state and transient state gas turbine operating conditions were considered, while the health parameters were continuously varied. To approximate practical situations, estimating health parameters under transient condition is more important.

In this section, the STEKF is applied for the gas turbine health parameter estimation and compared with the standard EKF and UKF considering three cases: (1) estimation error and computation cost analysis of the health parameters estimation approaches, (2) health parameter estimation under mutation condition, and (3) the effect of measurement noise on health parameter estimation.

In addition, ρ and β, two import parameters in the STEKF, need to be determined. Here, ρ $(0 < \rho \leq 1)$ is the forgetting factor and is usually selected as 0.95. The β $(\beta \geq 1)$ is the softening factor, which is used to soften the regulating strength of the λ_k and make the estimation smoother, and it can be selected empirically (Pu et al. 2013). In this study, $\rho = 0.95$ and $\beta = 10$ were selected for all the case studies.

5.1 Estimation Error and Computation Cost Analysis

In this section, the estimation error and computation cost analysis of the three nonlinear health parameter estimation approaches is described. The three Kalman filter approaches were applied to estimate the health parameters under 0.5%, 1%, 3%, and 5% decrease, and the gas turbine was in steady state at the design point. Table 4 shows the estimation results of the three estimation approaches for the compressor mass flow health parameters (H_{mc}) at four decreased amplitudes. The H_{mc} gradually decreased beginning at $t = 20$ s and reached the given amplitude at $t = 30$ s. The average of the estimated values from $t = 40$ s to $t = 50$ s was taken as the final estimation value. It can be seen that the three estimation approaches could accurately estimate the change of health parameters and the estimation error was small.

Figure 3 shows the estimation errors and variances of the three nonlinear filtering approaches, and the estimation error was calculated by $(|H_{act} - H_{est}|/ H_{act}) \times 100\%$. These figures show that the estimation errors of the three approaches decreased with the increase of the changing amplitude of the health parameters. The error and variance of the STEKF were similar to that of the EKF, while the UKF had the minimum estimation error and variance. This indicates that the estimation accuracies of the STEKF and EKF are similar but are less than the UFK estimation accuracy.

Figure 4 shows the health parameter estimation results for a 3% decrease in the compressor mass flow health parameter (H_{mc}) of the gas turbine, corresponding to the third column in Table 4. It can be seen that the health parameters estimation errors of the STEKF and the EKF were larger than that of the UKF; this is mainly because the UKF directly uses a gas turbine nonlinear model, which makes the UKF estimate accurate up to the third order (Simon, 2008), while the STEKF and the EKF need to be locally linearized, which makes them accurate up to the first order.

In addition, for the EKF, the estimated compressor turbine efficiency health parameter ($H_{\eta ct}$) increased as the compressor mass flow health parameter (H_{mc}) decreased by 3%, but in fact, the $H_{\eta ct}$ did not change. The possible reason for this result is that these health parameters may play a role in reducing the model error. To reduce the error between the model output and the actual measured value, the model error is compensated by adjusting the value of the health parameter, which leads to a change in the estimated value of these unchanged health parameters (Simon and Garg 2010). However, although the STEKF was also affected by the model uncertainty, its result was not like that of the EKF. This indicates that the STEKF is robust to model uncertainty; therefore, it can suppress the influence of model uncertainty on estimation results.

The computation costs of the three estimation approaches were also analyzed. All the case studies were modeled in the simulation platform using a 3.7 GHz PC with 8 GB RAM. For the case corresponding to Fig. 6, which had a simulation time of 60 s, three estimation approaches were used to estimate the health parameters, and the process was repeated ten times. The average computation costs for each approach is presented in Table 5. It can be seen that the computation costs of the

Table 4 Estimation results of three estimation approaches

Filter	Estimation of H_{mc} (%)			
Actual	−0.5	−1	−3	−5
STEKF	−0.510 ±0.045	−1.001 ±0.042	−2.998 ±0.035	−4.994 ±0.032
EKF	−0.499 ±0.042	−1.010 ±0.038	−3.003 ±0.033	−4.992 ±0.031
UKF	−0.493 ±0.011	−1.002 ±0.007	−2.998 ±0.013	−4.998 ±0.026

STEKF and EKF were approximate, and although the UKF had a high estimation accuracy, the corresponding computation cost was much greater than those of the STEKF and EKF.

5.2 Health Parameter Estimation Under Mutation Condition

The standard EKF loses the ability to track the health parameters when the gas turbine operates in mutation condition, resulting in an estimated delay (Zhou and Frank 1996). Therefore, in this section, the abilities of these three estimation approaches to track abruptly changing health parameters are compared. Figure 5 shows the estimated results of the three estimation approaches when the high-pressure turbine mass flow health parameters (H_{mct}) decreases by 3% at $t = 20$ s. In this case, the H_{mct} parameter abruptly decreases at $t = 20$ s, and the gas turbine is in steady state at the design point.

Figure 5 shows that the STEKF can quickly track the change of the health parameters when they change abruptly. When the health parameters changed, the estimated health parameters also changed rapidly and reached 3% at $t =$ 20.15 s. Due to the insensitivity to the mutation condition, the EKF estimation of the health parameters changed slowly, reaching 3% at $t = 21.2$ s. For the UKF, although the change of the health parameters could be quickly tracked, reaching 3% at $t = 20.85$ s, the estimation result fluctuated and took a long

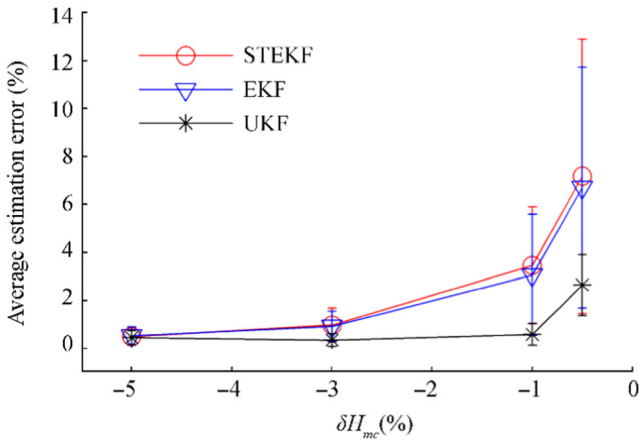

Fig. 3 Average estimation error and variance of the three estimation approaches for gradual decrease in H_{mc}

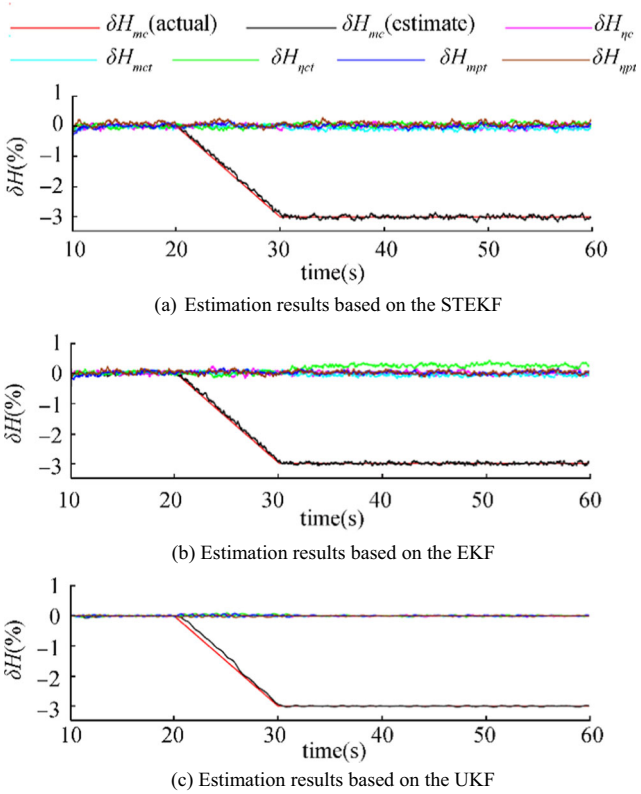

(a) Estimation results based on the STEKF

(b) Estimation results based on the EKF

(c) Estimation results based on the UKF

Fig. 4 Estimation results of the health parameter under gradual variation. **a** Estimation results based on the STEKF. **b** Estimation results based on the EKF. **c** Estimation results based on the UKF

time to stabilize. Therefore, the STEKF has a stronger health parameter mutation tracking ability than the standard EKF and UKF.

Figure 6 a shows the schedule of the gas turbine fuel flow w_f during the whole transient process of 40 s. The high-pressure turbine mass flow health parameter (H_{mct}) decreased by 3% at $t = 20$ s, and the estimation results of the three estimation approaches are shown in Fig. 6(b)–(d). It can be seen that when the health parameter mutation occurred in a transient condition, the STEKF could track the change of health parameters more quickly than the EKF and also had the strongest robustness to model uncertainty. Moreover, the estimation error of the high-pressure turbine efficiency health parameter ($H_{\eta ct}$) was much larger than those of other non-changing health parameters in the EKF, while the estimation error of the high-pressure turbine efficiency health parameter ($H_{\eta ct}$) was less for the STEKF. For the UKF, the mutation of the health

Table 5 Average computation costs of three estimation approaches after ten simulations

Approach	STEKF	EKF	UKF
Computation cost	9.27	9.25	89.82

parameter in a transition condition made the estimation result fluctuate and took a longer time to reach stability.

Figure 7 shows the estimation results of the three nonlinear estimation approaches for the simultaneous mutation change of multiple health parameters. In this case, the gas turbine was in steady state at the design point, and the efficiency health parameter ($H_{\eta c}$) and the mass flow health parameter (H_{mc}) of the compressor decreased by 3% at $t = 20$ s. The figure shows that the three nonlinear estimation approaches could accurately estimate the change of health parameters when multiple health parameters changed abruptly. The STEKF could estimate the change of health parameters most quickly; the estimated health parameters H_{mc} and $H_{\eta c}$ reached 3% at $t = 20.5$ s and $t = 20.43$ s, while for the EKF, the estimated parameters reached 3% at $t = 22.8$ s and $t = 24.9$ s. For the UKF, the parameters reached 3% at $t = 31.55$ s and $t = 26.35$ s; the UKF was most accurate, but its tracking ability was poor.

5.3 Effect of Measurement Noise on Health Parameter Estimation

In principle, the noise distribution has a great effect on the nonlinear Kalman filter estimation. In the conventional Kalman filter-based estimation approaches, the measurement noise is generally assumed as zero-mean Gaussian noise, but in practice, the mean noise value is not necessarily zero. In this section, the effects of the mean noise value on the performance of the three nonlinear estimation approaches are analyzed.

The standard deviation of noise relative to steady-state measurements are shown in Table 6 (Rahme and Meskin 2015). Figure 8 shows the average estimation error and the corresponding variance of the three estimation approaches in the case of the H_{mc} decrease by 3% at $t =$ 20 s when the gas turbine is in steady state at the design point. It can be seen that the estimation error corresponding to the EKF increased with the increase of the noise, indicating that the EKF performance was significantly affected by the mean noise value. However, the estimation errors corresponding to the STEKF and UKF were insensitive to the mean noise value, and the error of the STEKF was slightly larger than those of the UKF,

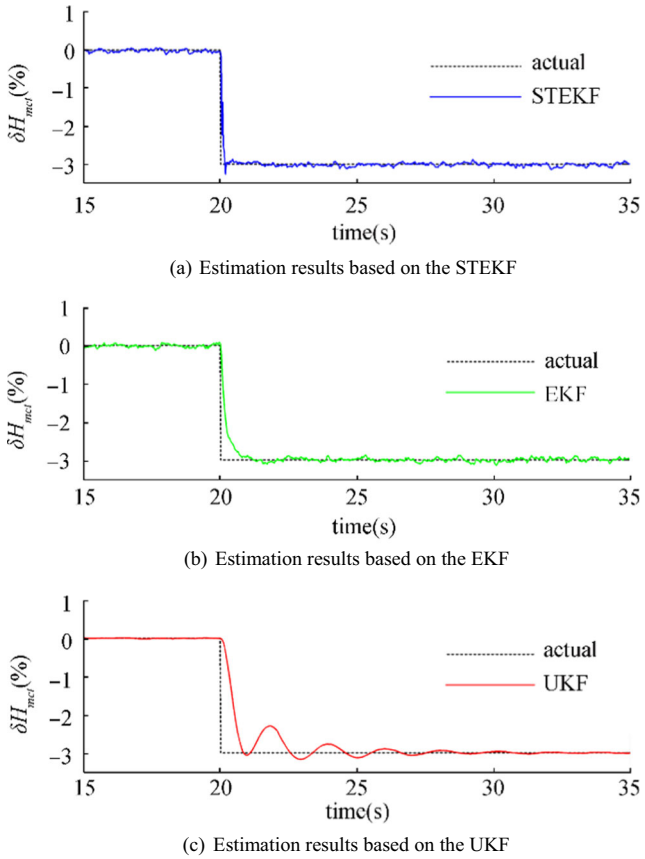

(a) Estimation results based on the STEKF

(b) Estimation results based on the EKF

(c) Estimation results based on the UKF

Fig. 5 Estimation results of the H_{mct} health parameter when H_{mct} changes abruptly. **a** Estimation results based on the STEKF. **b** Estimation results based on the EKF. **c** Estimation results based on the UKF

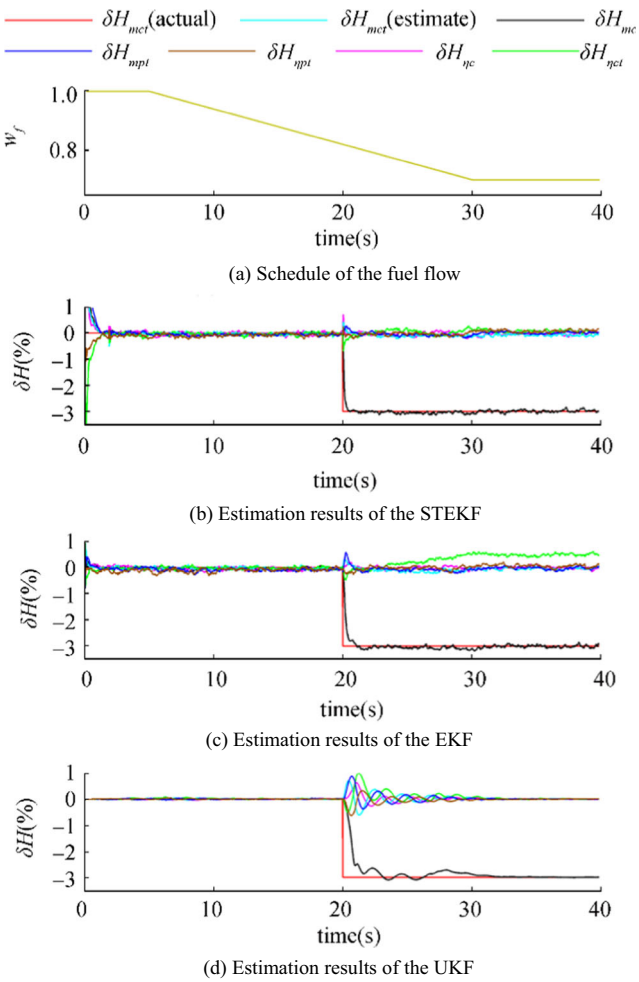

(a) Schedule of the fuel flow

(b) Estimation results of the STEKF

(c) Estimation results of the EKF

(d) Estimation results of the UKF

Fig. 6 Estimation results of the H_{mct} health parameter under transient condition. (**a**) Schedule of the fuel flow. (**b**) Estimation results of the STEKF. (**c**) Estimation results of the EKF. (**d**) Estimation results of the UKF

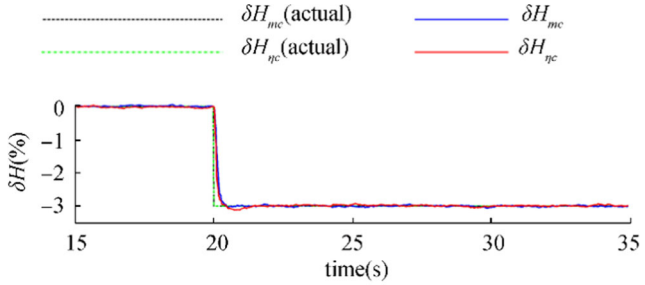

(a) Estimation results of the STEKF

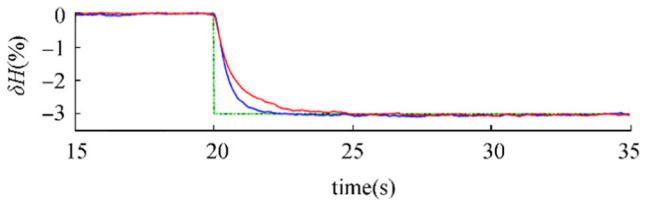

(b) Estimation results of the EKF

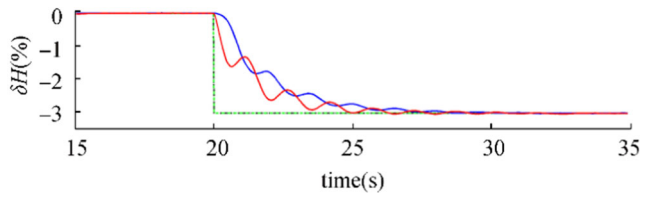

(c) Estimation results of the UKF

Fig. 7 Estimation results of H_{mc} and $H_{\eta c}$ health parameters when H_{mc} and $H_{\eta c}$ change abruptly. (**a**) Estimation results of the STEKF. (**b**) Estimation results of the EKF. (**c**) Estimation results of the UKF

indicating that the STEKF outperformed the EKF when the mean noise was not zero. Figure 9 shows the estimation results of the health parameter when the mean value of the noise was 0.1. As seen, the STEKF and UKF could still accurately estimate the fault amplitude, but the STEKF had a stronger tracking ability than the UKF. However, affected by the non-zero-mean value of the noise, the EKF estimation of H_{mc} and H_{mpt} showed a large error.

In addition, the effects of noise variance on the performance of the three estimation approaches were also analyzed. Figure 10 shows the average estimation error and variance of the approaches when the variance of the noise increases. It can be seen that the estimation errors for the STEKF and the EKF increased with the increase of noise variance, and the estimation accuracies of both were approximate. In addition,

Table 6 Standard deviation of noise relative to steady-state measurements (%)

Measurement parameters	N_l	N_p	T_2	P_2
Standard deviation (%)	0.051	0.051	0.23	0.164
Measurement parameters	T_4	P_4	T_5	P_5
Standard deviation (%)	0.097	0.164	0.097	0.164

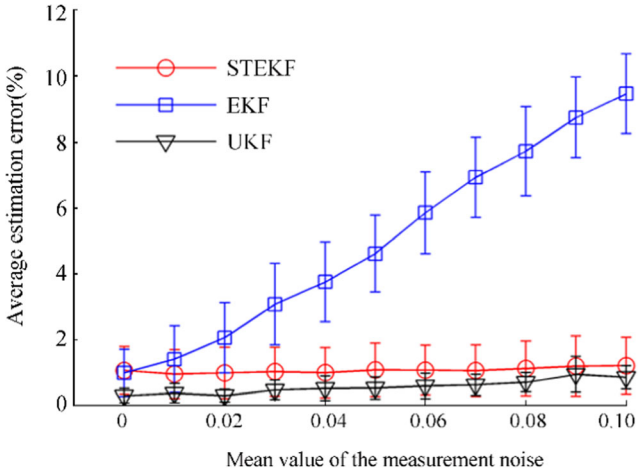

Fig. 8 Average estimation error and variance of the three estimation approaches when the mean noise value changes

although the estimation performance of the UKF was better than those of the STEKF and EKF both in the situations of increase in mean noise and noise variance, its computation cost was much greater than those of the other two approaches, as shown in Table 5.

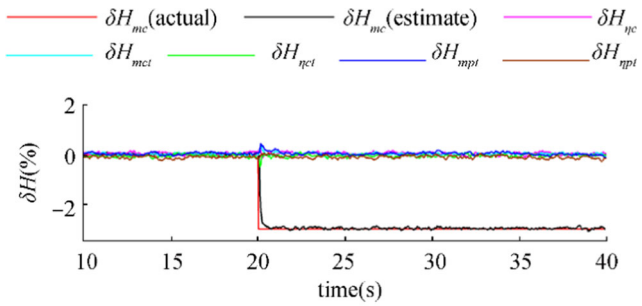

(a) Estimation results based on the STEKF

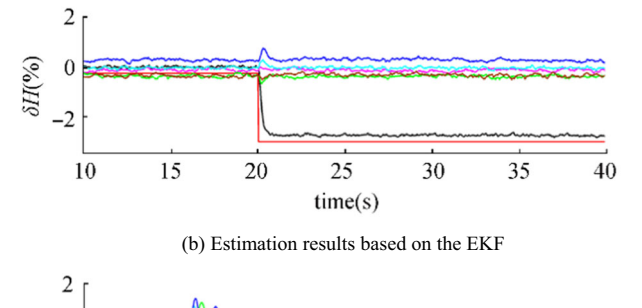

(b) Estimation results based on the EKF

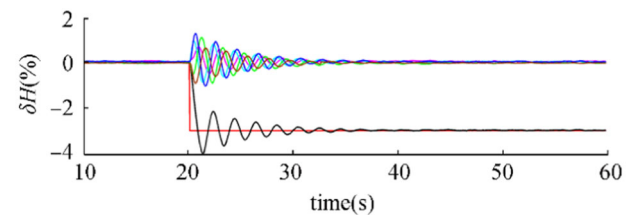

(c) Estimation results based on the UKF

Fig. 9 Estimation results of the health parameter when the mean noise value is 0.1. (**a**) Estimation results based on the STEKF. (**b**) Estimation results based on the EKF. (**c**) Estimation results based on the UKF

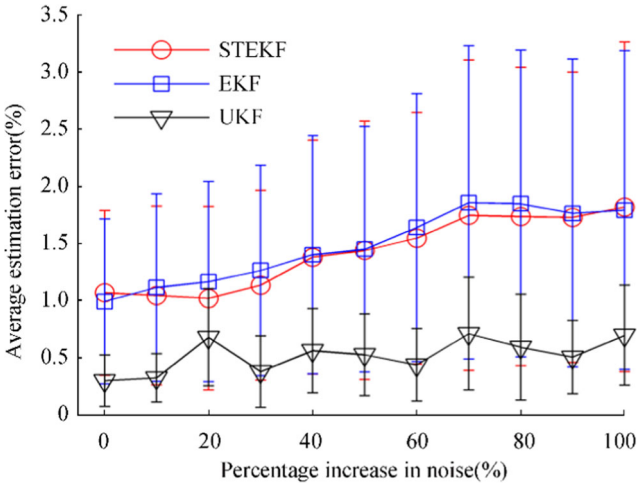

Fig. 10 Average estimation error and variance of the three estimation approaches when the noise variance increases

6 Conclusion

In this paper, to overcome the problem of poor tracking ability under mutation condition and poor robustness to model uncertainties, an improved Kalman filter-based algorithm called the STEKF was proposed to estimate the gas turbine health parameters, and the algorithm was compared with the commonly used EKF and UKF. Several case studies were considered for the modeling of a two-shaft marine gas turbine engine in a simulation environment. The results show that the proposed STEKF approach not only has a computation cost similar to that of the EKF approach and much shorter than that of the UKF, but is also robust to model uncertainties caused by local linearization and outperforms the EKF approach when the noise mean value increases. In addition, whether in steady or transient state, single fault or multiple faults, the proposed STEKF approach has a stronger ability to track the mutational health parameters than the EKF and UKF approaches.

References

Borguet S, Léonard O (2010) Comparison of adaptive filters for gas turbine performance monitoring. Journal of Computational & Applied Mathematics 234(7):2202–2212. https://doi.org/10.1016/j.cam.2009.08.075

Brotherton T, Volponi A, Luppold R, Simon DL (2003) eSTORM: enhanced self-tuning on-board real-time engine model. In: Proceedings of the 2003 IEEE aerospace conference, Big Sky, 3075–3086. https://doi.org/10.1109/AERO.2003.1234150

Camporeale SM, Fortunato B, Mastrovito M (2006) A modular code for real time dynamic simulation of gas turbines in Simulink. J Eng Gas Turbines Power 128(3):506–517. https://doi.org/10.1115/1.2132383

Chang X, Huang J, Lu F, Sun H (2016) Gas-path health estimation for an aircraft engine based on a sliding mode observer. Energies 9(8):598. https://doi.org/10.3390/en9080598

Johansen TA, Hunt KJ, Gawthrop PJ, Fritz H (1998) Off-equilibrium linearisation and design of gain-scheduled control with application to vehicle speed control. Control Eng Pract 6(2):167–180. https://doi.org/10.1016/S0967-0661(98)00015-X

Kerr LJ, Nemec TS, Gallops GW (1992) Real-time estimation of gas turbine engine damage using a control-based Kalman filter algorithm. J Eng Gas Turbines Power 114(2):187–195. https://doi.org/10.1115/1.2906571

Klapproth J, Miller M, Parker D (1979) Aerodynamic development and performance of CF6-6/LM2500 compressor. In: Proceedings of 4th international symposium on air breathing engines, Orlando, 243–249. https://doi.org/10.2514/6.1979-7030

Kobayashi T, Simon DL, Litt JS (2005) Application of a constant gain extended Kalman filter for in-flight estimation of aircraft engine performance parameters. In: Proceedings of ASME Turbo expo 2005: power for land, sea, and air, Reno, 617–628. https://doi.org/10.1115/GT2005-68494

Lambert HH (1991) A simulation study of turbofan engine deterioration estimation using Kalman filtering techniques. NASA Technical Memorandum 104233

Li YG (2010) Gas turbine performance and health status estimation using adaptive gas path analysis. J Eng Gas Turbines Power 132(4):109–121. https://doi.org/10.1115/1.3159378

Li YG, Korakiantis T (2012) Nonlinear weighted least squares estimation approach for gas-turbine diagnostic applications. Journal of Propulsion & Power 27(2):337–345. https://doi.org/10.2514/1.47129

Li YG, Pilidis P (2010) Ga-based design-point performance adaptation and its comparison with icm-based approach. Appl Energy 87(1):340–348. https://doi.org/10.1016/j.apenergy.2009.05.034

Lu F, Huang J, Lv Y (2013) Gas path health monitoring for a turbofan engine based on a nonlinear filtering approach. Energies 6(1):492–513. https://doi.org/10.3390/en6010492

Luppold RH, Roman JR, Gallops GW (1989) Estimating in-flight engine performance variations using Kalman filter concepts. *Proceeding of the 25th AIAA/ASME/SAE/ASEE Joint Propulsion Conference*, Monterey, 1–10. https://doi.org/10.2514/6.1989-2584

Pu X, Liu S, Jiang H, Yu D (2013) Adaptive gas path diagnostics using strong tracking filter. Proc IMechE, Part G: Journal of Aerospace Engineering 228(4):577–585. https://doi.org/10.1177/0954410013478514

Rahme S, Meskin N (2015) Adaptive sliding mode observer for sensor fault diagnosis of an industrial gas turbine. Control Eng Pract 38:57–74. https://doi.org/10.1016/j.conengprac.2015.01.006

Simon D (2006) H_∞ filtering with inequality constraints for aircraft turbofan engine health estimation. In: Proceedings of the 45th IEEE conference on decision and control, San Diego, CA, 3291–3296. https://doi.org/10.1109/CDC.2006.376880

Simon D (2008) A comparison of filtering approaches for aircraft engine health estimation. Aerosp Sci Technol 12(2):276–284. https://doi.org/10.1016/j.ast.2007.06.002

Simon DL, Garg S (2010) Optimal tuner selection for Kalman filter-based aircraft engine performance estimation. J Eng Gas Turbines Power 132(3):659–671. https://doi.org/10.1115/GT2009-59684

Simon D, Simon DL (2005) Aircraft turbofan engine health estimation using constrained Kalman filtering. J Eng Gas Turbines Power 127(2):323–328. https://doi.org/10.1115/1.1789153

Simon D, Simon DL (2006) Kalman filter constraint switching for turbofan engine health estimation. Eur J Control 12(3):331–343. https://doi.org/10.3166/ejc.12.341-343

Simon D, Simon DL (2010) Constrained Kalman filtering via density function truncation for turbofan engine health estimation. Int J Syst Sci 41(2):159–171. https://doi.org/10.1080/00207720903042970

Tsoutsanis E, Meskin N, Benammar M, Khorasani K (2013) Dynamic performance simulation of an aeroderivative gas turbine using the Matlab Simulink environment. In: Proceedings of ASME 2013

international mechanical engineering congress and exposition, San Diego, CA, 1–10. https://doi.org/10.1115/IMECE2013-64102

Volponi AJ (2013) Gas turbine engine health management: past, present and future trends. J Eng Gas Turbines Power 58(136):433–455. https://doi.org/10.1115/1.4026126

Volponi A, DePold H, Ganguli R, Daguang C (2003) The use of Kalman filter and neural network methodologies in gas turbine performance diagnostics: a comparative study. J Eng Gas Turbines Power 125(4): 917–924. https://doi.org/10.1115/2000-GT-0547

Yang X, Shen W, Pang S, Li B, Jiang K, Wang Y (2014) A novel gas turbine engine health status estimation approach using quantum behaved particle swarm optimization. Math Probl Eng 2014(3):1–11. https://doi.org/10.1155/2014/302514

Yang Q, Li S, Cao Y (2017) A new component map generation method for gas turbine adaptation performance simulation. Journal of Mechanical Science & Technology 31(4):1947–1957. https://doi.org/10.1007/s12206-017-0344-5

Zhou DH, Frank PM (1996) Strong tracking Kalman filtering of nonlinear time-varying stochastic systems with coloured noise: application to parameter estimation and empirical robustness analysis. Int J Control 65(2):295–307. https://doi.org/10.1080/00207179608921698